LATER but FORTIOR: diffusion modelling of inhibition of return

Tal Seidel Malkinson[1↓], Alexia Bourgeois [2], Nicolas Wattiez[3], Pierre Pouget[1*] and Paolo Bartolomeo[1*]

1. Sorbonne Université, Inserm UMRS 1127, CNRS UMR 7225, Paris Brain Institute, ICM, Hôpital de la Pitié-Salpêtrière, F-75013 Paris, France
2. Laboratory of Cognitive Neurorehabilitation, Faculty of Medicine, University of Geneva, 1206 Geneva, Switzerland.
3. Sorbonne Université, INSERM UMRS 1158 Neurophysiologie Respiratoire Expérimentale et Clinique, F-75005 Paris, France

↓ corresponding author

* these authors contributed equally to this work

Abstract

Inhibition of return (IOR) refers to the slowing of response times (RTs) for stimuli repeated at previously inspected locations, as compared with novel ones. However, the exact processing stage(s) at which IOR occurs, and its nature across different response modalities, remain debated. We tested predictions on these issues originating from the FORTIOR model (fronto-parietal organization of response times in IOR; Seidel Malkinson & Bartolomeo, 2018), and from accumulator models such as LATER (linear approach to threshold with ergodic rate; Carpenter & Williams, 1995). We reanalysed RT data from a target-target IOR paradigm (Bourgeois et al., 2013a, 2013b) by using a Linear Ballistic Accumulator model, to test the predictions of FORTIOR, and specifically whether IOR could occur at early sensory/attentional stages of processing, or at later stages of decision and action selection. We considered the following conditions: manual or saccadic response modality, before or after TMS perturbation over four cortical regions. Results showed that the slope parameter best explained both manual and saccadic IOR, suggesting that in both response modalities IOR may result from slower accumulation of evidence for repeated locations. Additionally, TMS stimulation over the right intra-parietal sulcus (IPS) affected the model's goodness of fit, and the slope parameter best explained the perturbed manual IOR, suggesting that the right IPS might be involved in the accumulation of evidence towards a decision. TMS perturbation over regions that did not affect IOR, nonetheless significantly decreased the goodness of fit of manual IOR models in a nonspecific manner, suggesting that TMS increases intra-individual RT variability. These results support the hypothesis that IOR is a predominantly sensory/attentional phenomenon, and is modulated by activity in fronto-parietal networks.

Introduction

Inhibition of return (IOR) refers to the slowing of response times (RTs) for stimuli repeated at previously inspected locations, as compared with novel ones (Berlucchi et al., 1981; Klein & Redden, 2018; Lupiáñez et al., 2006; Posner & Cohen, 1984). IOR is believed to promote our exploration of the environment by avoiding repeated scanning of previously visited locations (Klein, 1988). This phenomenon was extensively explored since its discovery in the ’80s, but its exact nature and neural bases remain debated. Repeated peripheral events can result in faster RTs (facilitation) or slower RTs (IOR), depending on several variables, including the delay between the stimuli, the motor effector used (manual responses or eye saccades), and the type of visual task (detection or discrimination) (Lupiáñez, 2010). As noted by some theorists (Berlucchi, 2006; Lupiáñez, 2010), this evidence challenges the view of IOR as the result of inhibiting attention from returning to a previously explored location (Klein & Redden, 2018; Posner et al., 1985). In addition, the neural bases of IOR, as well as the exact processing stage(s) of IOR generation are currently unclear. IOR could occur at early sensory/attentional stages of processing, or at later stages of decision and action control. Originally, Posner et al. (1985) had suggested the cause for IOR was the orienting of attention towards a location and the subsequent removal of attention from that location, to discourage attention from re-orienting back to the originally attended location. However, this explanation was found to be lacking, and that oculomotor programming has an important contribution to IOR generation (See Klein, 2000 for a review). Converging evidence suggests that IOR could delay both motor responses and the return of attention (Lupiáñez et al., 2006).

Correspondingly, several subcortical and cortical regions were shown to be implicated in the generation of IOR. For example, neuropsychological evidence (Sapir et al., 1999) and non-human primate electrophysiology (Dorris et al., 2002) suggest an important role for the midbrain superior colliculus (SC), though the SC is not the site where the inhibition is generated (Dorris et al., 2002). Dorris et al suggested that a potential inhibition-generation site could be the posterior parietal cortex (PPC). Supporting evidence for this hypothesis comes from electrophysiological studies showing that neural activity in monkey LIP was found to be reduced for already explored targets in visual search (Mirpour et al., 2009). Further evidence comes from the observation that in human patients with right hemisphere damage and visual neglect, manual IOR was reduced for right-sided, non-neglected repeated stimuli (Bartolomeo et al., 1999, 2001), where it could even revert to a “facilitation of return”, ie faster RTs for repeated targets (Bourgeois et al., 2012). An advanced lesion analysis in the Bourgeois et al.’s (2012) study showed that facilitation of return was found in patients with damage either to the supramarginal gyrus in the right parietal lobe, or to its connections with the ipsilateral prefrontal cortex. Importantly, however, these patients showed normal saccadic IOR.

One way to explore the causal role of the suggested underlying brain structures in the generation of IOR is by applying transcranial magnetic stimulation (TMS) (Satel et al., 2019). In a series of

studies, Bourgeois et al. (2013a, 2013b) used repetitive TMS to test the causal role of distinct nodes of the human fronto-parietal attention networks in the generation of manual and saccadic IOR in a target-target paradigm (see Maylor & Hockey, 1985). Critically, transient interference of the intra-parietal sulcus (IPS) and temporo-parietal junction (TPJ) in either hemisphere affected IOR differently, and these effects were hemifield- and effector-dependent. Specifically, rTMS over the right hemisphere TPJ interfered with IOR only for manual responses with ipsilateral (right) targets, consistent with data obtained in right-brain damaged patients with neglect (Bourgeois et al., 2012). TMS over the right hemisphere IPS perturbed manual IOR for targets on both sides of the screen, but saccadic IOR was affected only for contralateral (left) targets (Bourgeois et al., 2013b). Left hemisphere stimulation did not affect IOR (Bourgeois et al., 2013a). More recently, Seidel Malkinson & Bartolomeo (2018) proposed a theoretical model labeled FORTIOR (Frontoparietal Organization for Response Times in IOR), to explain the cortical basis of IOR generation in target-target detection paradigms, and to account for the complex pattern of interference produced by TMS stimulation. Based on the known architecture of frontoparietal cortical networks and on their anatomical and functional asymmetries (Bartolomeo & Seidel Malkinson, 2019), FORTIOR postulates that both manual and saccadic IOR arise from reverberation of activity within priority maps of the frontoparietal circuit linking frontal eye field (FEF) and intraparietal sulcus (IPS). Differences between the readout capacities of the manual and saccadic effector systems when reading the output of the FEF-IPS circuit may then lead to the dissociations between saccadic and manual IOR. Klein and Redden (2018) suggested a different view, and proposed the existence of two types of IOR: an 'input' form causing IOR by biasing perception, and an 'output' form causing IOR by biasing action. Specifically, Klein and Redden suggested that input-IOR is generated when the reflexive oculomotor system is actively suppressed (ie, when participants must maintain fixation and respond manually), and results from modulation of activity in early sensory pathways in retinotopic coordinates, rather than from response outputs. Output-IOR occurs when the reflexive oculomotor system is not suppressed, and involves projections from the SC to cortical areas (i.e. FEF and PPC). Output IOR is spatiotopic and is independent of the response modality. Therefore, according to this account, manual IOR (while maintaining fixation) and saccadic IOR reflect different inhibitory processes and implicate different underlying neural mechanisms.

Accumulator models, which explain the decision to respond as an accumulation of evidence to a response threshold (see also reviews by Duncan Luce, 1986; Ratcliff & Smith, 2004), can provide an important contribution to our understanding of IOR. Both behavioural and neurophysiological evidence suggest that the accumulation rate is affected by the stimulus quality and that the evidence criterion is modulated by the prior probability of a particular response (Gold & Shadlen, 2007; Pouget et al., 2011). In the case of IOR, increased RTs for repeated targets might be explained by a variety of model parameters (Satel et al., 2019), such as sensory-level effects (e.g., slower rate of accumulation or decreased noise), or a later decision-level effect (higher decision threshold). The identification of the relevant parameters may thus help determine the processes implicated in IOR. Presently, only two studies used this approach to explore IOR. The first one

modelled RT data from two experiments, in which participants generated sequences of three saccades in response to a peripheral or a central cue, generating saccadic IOR for movements to the immediately preceding fixated location (Ludwig et al., 2009). Saccadic IOR was best accounted for by a change in the accumulation rate. Ludwig et al. (2009) concluded that an attenuated sensory response to stimulation at a recently fixated location might be responsible for a lower accumulation rate for a response to that location. This finding was the first to propose a plausible explanation for a reduced accumulation rate under peripheral cueing conditions. However, the authors did not extend their finding to manual responses, and therefore could not provide evidence of such an account for the data produced with a non-specific effector (see also Rafal et al., 1994; Taylor & Klein, 2000).

In the second study, MacInnes (2017) modelled data from two experiments testing the gradient of IOR with random, continuous cue-target Euclidean distance and cue-target onset asynchrony. Although the behavioral RTs differed across response modalities, best-fit models were shown to have similar model parameters for the gradient of IOR for both effector types, suggesting similar underlying mechanisms for saccadic and manual IOR. Contrary to Ludwig et al. (2009), MacInnes (2017) found that the model parameter best explaining location-associated changes in RT was the variance of accumulation starting point for both manual and saccadic responses. When the spatial distance between the location of the cue and the target increases, the variability in the starting point of information accumulation also increases. This, on average, shifts the accumulation closer to the decision threshold and thus decreases RTs. This result is consistent with neural results where changes in resting state activation levels in SC (Dorris & Munoz, 1998) are dependent on target location probabilities. The conflicting results of IOR-associated model parameters in the Ludwig et al. (2009) and MacInnes (2017) studies may result from differences in the experimental paradigm. However, in both cases the modelling procedure fitted only one parameter at a time and did not simultaneously compare the fit of these two parameters.

To address these issues, here we used the accumulation model LATER (linear approach to threshold with ergodic rate; Carpenter & Williams, 1995; see also for review Noorani, 2014; Schall, 2019). Conceptually minimalist and mathematically tractable, LATER is a simple model for RTs. According to LATER, information linearly accumulates until reaching a criterion. Accumulation rate distribution is Gaussian and its starting point is uniformly distributed. A simple and formal view of this model is illustrated in Figure 2 below, which shows what may be regarded as the 'decision period' of a fixation period prior to saccadic or manual initiation response. An additional, constant non-decisional latency that includes afferent and efferent delays associated with stimulus encoding and peripheral motor delays is also added to 'the decision period' (Brown & Heathcote, 2008; Pouget et al., 2009). In LATER, a decision signal starts from a starting point S_0 and rises toward a threshold θ. Once the signal reaches the threshold, a decision is made for a particular action. The rate at which the decision signal rises varies randomly from trial to trial, but the mean rate of rise is constant and denoted by the parameter μ. The standard deviation of this variation in rate of rise is given by the parameter σ (see Figure 2). Together, these

assumptions of variability in starting point and accumulation rate are sufficient to produce latency distributions that have the appropriate typical right-skewed shape.

In the present study, we used LATER to further explore the mechanism of IOR, the dissociation between saccadic and manual IOR, and the nature of TMS-induced IOR perturbations. Specifically, we had three aims: 1. Determine if IOR RT-distributions could be best accounted for by sensory parameters (rate of accumulation and noise), or by decisional processes (decision threshold); 2. Test whether RT-distributions for manual and saccadic IOR can be fitted with the same model parameters, and thus reflect a common mechanism; 3. Explore if TMS-induced IOR perturbation operates at a sensory or a decisional level.

Methods

Experimental data

The RT data used for modelling was taken from the studies by Bourgeois et al. (2013a, 2013b), who used repetitive TMS to assess the causal role of distinct nodes of the human frontoparietal networks in attentional orienting. In these studies, participants performed a target-target paradigm (see Maylor & Hockey, 1985). Four black peripheral circles surrounding a circle placed at fixation were displayed. Participants had to respond as fast as possible to one of the peripheral circles becoming white, either by pressing a key while maintaining fixation, or, in a different session, by making a saccade towards the target. We compared RTs for targets appearing at the same location of the preceding one (Return trials) with RTs for targets appearing at new locations at the horizontally and vertically opposite side of the display (ie, a bottom-left target after a top-right target; Non-return trials). Responses to right-sided and left-sided targets were pooled together inside each return category to maximize modelling robustness. The TMS-stimulated brain nodes were the intraparietal sulcus (IPS) and the temporo-parietal junction (TPJ) in the left or in the right hemisphere.

Model fitting

The race model is composed of a simple go unit. His activity is governed by a stochastic differential equation (Usher & McClelland, 2001) with a null leakage factor:

$$dago(t) = dago(t-1) + \mu go + \xi go$$

The unit is defined by two parameters: the mean growth rate (μ) and a Gaussian noise term (σ) with a mean of zero variance of σ2go, where a represents the activity of the unit. The race finished when the unit crossed the threshold (θ), within a limit of 3000 ms. If unit activity is negative during the race, the activity was reset to zero at this point (non-physiologic value). An

additional parameter, Dgo, was added to the model to take into account the stimulus encoding that occurred in the go unit. Dgo was set to 100 ms. μ, σ and θ are the unconstrained parameters of the model.

The observed latency distributions for correct responses as the latency distributions generated by the model were binned into 5 quantiles, defined by the following boundaries: {0, 0.2, 0.4, 0.6, 0.8, 1.0}. A local chi-square was computed at each bin and a general chi-square was obtained by summing each local chi-square. To find the best parameters for each latency distribution, we minimized the general chi-square by using a minimization function (patternsearch from the global optimization toolbox of Matlab). Patternsearch looks for a minimum based on an adaptive mesh that is aligned with the coordinate directions. Because minimization functions are sensitive to their starting point, we ran pattern search from 50 randomly chosen starting points. Finally, to avoid a local minimum, we again started patternsearch from 200 new start points. These starting points were determined by the best parameters from the first run and were defined as follows: best parameters ± 0.01 units and best parameters ± 0.02 units. After applying this procedure to each distribution of the Return and the Non Return conditions, we ran a new procedure in order to determine which of the μ, σ or θ parameter could explain the differences observed in the Return and the Non-Return latency distributions. To do this, we fixed two parameters of the Return condition on latency distribution of the Non-return condition and let one parameter free. As in the first procedure, pattern search was run from 50 randomly chosen starting points and then from 200 new start points. All these procedures were performed on a supercomputer cluster (NEC, 40 nodes, 28 cpu Intel Xeon E5-2680 V4 2.4 GHz/node, 128 Go RAM/node).

Statistical analysis

RTs and model parameters derived from the LATER models were statistically compared using the JASP software (Jasp Team, 2020, JASP (Version 0.12)[Computer software]). In order to keep inter- and intra-subjects RT variability, only trials with RTs shorter than 100ms (anticipations) were excluded. This trial selection allowed us to estimate Gaussian noise parameters without a priori in RT distributions and maximize the number of trials entered into the models. For RT analysis, these same trial-selection criteria were used. This selection includes 3-10% of highly variable latency especially in TMS condition (see TMS Results section). Based on this trial selection, only subjects whose model goodness of fit was smaller than 2 SD of the mean fit per each condition were included in the analysis. The included participants were 28 (78% of initial sample) for the manual response condition, and 31 (86% of initial sample) for the saccadic response condition; 24 (86% of initial sample) for the left IPS, left TPJ and right TPJ TMS condition; N=7 (88% of initial sample) for the right IPS TMS condition. The present trial selection procedure thus differs from the one originally used by Bourgeois et al. (2013a, 2013b), where outlier RTs were excluded and data for right-sided and left-sided targets could be separately analysed. The mean RTs per condition of subjects that were included in at least one of the modelling conditions analysis were computed and included in the analysis of RTs (N=33). When possible, repeated measures ANOVAs

(with Greenhouse-Geisser correction when necessary) and Bonferroni-corrected post hoc tests were used for RT and model parameter analyses. For the right IPS condition, non-parametric Friedman and Durbin tests were performed, followed by Conover's post hoc tests. Non-significant differences in the post hoc tests between All free parameters and Single free parameter models were assessed for potential equivalence by using Equivalence Bayesian Paired Samples t-test (Gronau et al., 2019).

Results

Across subjects, the median number of included trials for manual responses was 32.5 (range, 18-50) and 34 for saccadic responses (range, 24-76), after excluding anticipatory responses. This group of responses itself is distributed across the two conditions (Return vs Non-return), so that the number of included responses for any one type of sequence ranged from 18 to 76. Fig. 1 shows the mean saccade latencies and manual response times across subjects, for each of the conditions of Return vs Non-return, TMS and no TMS. A number of strong trends emerge. First, a three factor repeated-measures ANOVA was performed to assess the reliability of the Return and TMS across both manual and saccades conditions. The main effect of Return versus Non-return was significant ($F_{(1,33)}$=8.34, p=0.004, η^2=0.01; see figure 1). There was no interaction between Return and the other two factors, suggesting that IOR was independent of response modality and TMS application, presumably because our more liberal trial selection procedure limited the subtlety of the effects we could observe as compared with the original studies by Bourgeois et al. (2013a, 2013b) (see Statistical analysis in the Methods section). TMS and response modality interacted ($F_{(1,33)}$=6.89, p=0.013, η^2=0.04), because only manual response were affected by TMS (Post hoc tests: Saccadic response pre TMS VS post TMS: p=1; Manual response pre TMS VS post TMS: p=0.039). In Fig. 2, Reciprobit plots correspond to the loglog cumulative probability distribution. Each dot represents a manual or saccadic response in Return (black) or Non-return (grey) conditions. The left inset shows the optimal model fits with adjustment of each parameter (from top to bottom: with μ, σ and θ adjustments). The right part of each panel illustrates an example of a single session showing RT variations better fitted with a single parameter adjustment (respectively μ, σ or θ; from top to bottom). The figure shows the mean accumulation rates estimated in the model fits; mean rates are plotted separately for Return and Non-return response (Black and grey line respectively). If IOR is mediated by a change in the underlying rate of accumulation, the rate should be lower for Return responses compared to Non-return responses. If IOR reflects the need for more evidence, the threshold should be elevated for Return responses. The mean accumulation rate for Return responses is, on average, lower than that for Non-return responses.

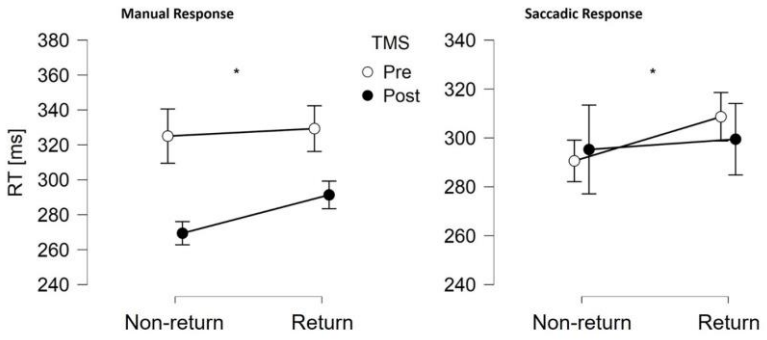

Figure 1: Response time inhibition of return (IOR) effect: Manual response time (RT, left panel) and Saccadic RT (right panel) are longer in Return trials than in Non-return trials (Return main effect, p=0.007), pre TMS perturbation (white circles) and post TMS perturbation (black circles). TMS perturbation affects manual responses more than saccadic responses (TMS X Response modality interaction, p=0.013). Error bars represent SE.

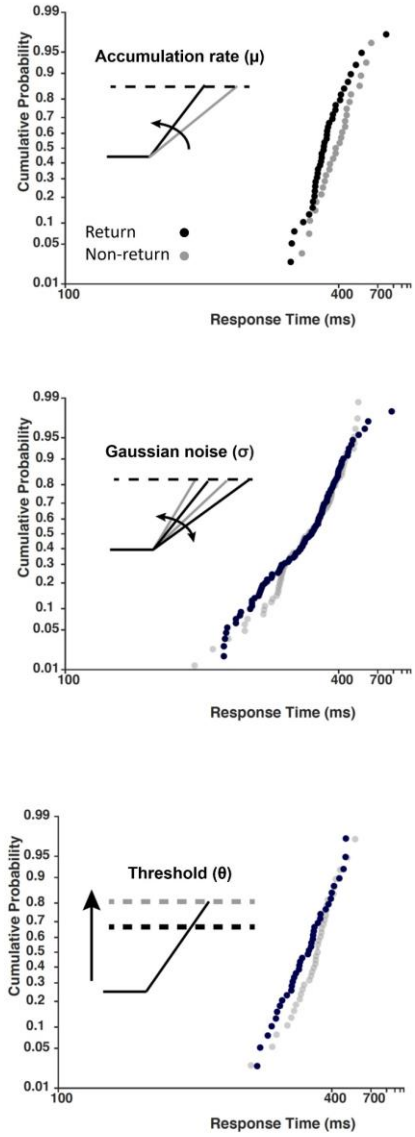

Figure 2: Reciprobit response time distributions for Return (black dots) and Non-return (grey dots) trials. Inset illustrates the model parameter accounting for response time differences due to inhibition of return (IOR). Race to threshold between two independent accumulators, each subject to Gaussian variability in the accumulation rate and uniform variability in the starting point of accumulation. The accumulator coding the Return condition is shown by the black line. The Non-return condition is coded by the grey accumulators. (Top panel) The target is at a Return location, causing a reduction in the accumulation rate of the associated movement program. As a result, the threshold is crossed later. (Middle panel) The target is at a return location (black dots), resulting in a selective increased variability in the accumulation rate of the accumulator coding the target and a delay in the time at which the threshold is reached. (Lower panel) The target is at a return location, resulting in a selective increase in the evidence criterion for the accumulator coding the target and a delay in the time at which threshold is reached.

Manual IOR is explained by the Slope parameter

Manual RTs of Return trials and Non-return trials were separately fit with accumulator models with 3 free parameters. The resulting Return condition model parameters were then used to constrain the Non-return model fit, thus allowing to explore which parameter best accounted for the differences between Return and Non-return trials caused by IOR. A repeated measures ANOVA with main factor of Model Goodness of fit (four levels: All free parameters, μ free, σ free and θ free models), showed a significant main effect ($F_{(1.69,45.75)}$=21.21, p<0.001, η^2=0.44; see Figure 3), resulting from significant differences between the fit of the All free parameters model and the σ free and θ free models (Post Hoc comparisons: p=0.032, p<0.001, respectively). The difference between the fit of the μ free model and the All free parameters model did not reach significance (post hoc comparisons: p=1). Equivalence Bayesian Paired Samples t-test showed that there was not enough evidence to support or reject the equivalence of the fit between these two models (overlapping-hypothesis Bayes Factor [BF] in favor of the interval-null=0.99; non overlapping-hypothesis BF in favor of the interval-null=0.98). There was no significant correlation between manual IOR effect and either of the model parameters. These results suggest that changes in the rate of accumulation best explain RT differences between Return and Non-return trials, and thus support a perceptual/attentional account of manual IOR.

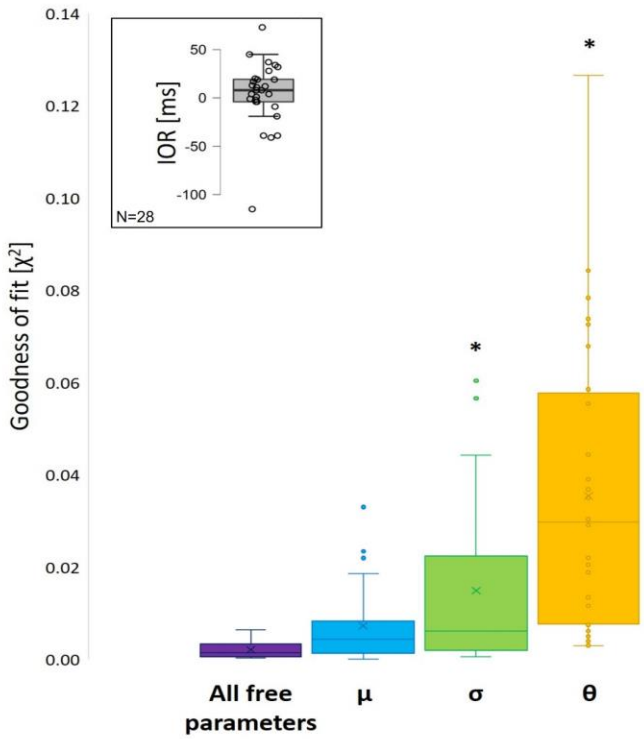

Figure 3: Manual IOR effect is explained by the Slope parameter. A. The goodness of fit of the All free parameters model (Purple) significantly differed from the fit of the Gaussian noise free parameter model (σ, green) and the Threshold free parameter model (θ, yellow) (repeated measures ANOVA, p<0.001, post hoc tests p=0.03, p<0.001 respectively), suggesting that the Slope free parameter (μ, blue) differs between Return and Non-return conditions. Inset: The manual IOR effect of the subjects included in the modeling.

Saccadic IOR is explained by the Slope parameter

Manual RTs of Return trials and Non-return trials were separately fit with accumulator models with three free parameters. The resulting Return condition model parameters were then used to constrain the Non-return model fit, thus allowing to explore which parameter best accounted for the differences between Return and Non-return trials caused by IOR. A repeated measures ANOVA with main factor of Model Goodness of fit (four levels: All free parameters, μ free, σ free and θ free models), showed a significant main effect ($F_{(2.12,63.51)}$=13.68, p<0.001, η^2=0.31; see Figure 4), resulting from significant differences between the fit of the All free parameters model and the σ free and θ free models (Post Hoc comparisons, all ps<0.001). The difference between the fit of the μ free model and the All free parameters model did not reach significance (post hoc comparisons, p=0.1). Equivalence Bayesian Paired Samples t-test showed moderate to strong evidence in favor of the equivalence of the fit between these two models (overlapping-hypothesis BF in favor of the interval-null, 2.26; non overlapping-hypothesis BF in favor of the interval-null, 12.03). We then tested the association between model parameters and saccadic IOR. We found that the μ and the σ model parameters, but not the θ parameter, were significantly correlated with saccadic IOR (Spearman correlations: $\rho_{(\text{saccadic IOR},\mu)}$=0.38, p=0.036; $\rho_{(\text{saccadic IOR},\sigma)}$=0.58 p<0.001; $\rho_{(\text{saccadic IOR},\theta)}$=0.16, p=0.39). These results suggest that accumulation rate and its variability best explain RT differences between Return and Non-return trials, consistent with a perceptual/attentional account of saccadic IOR.

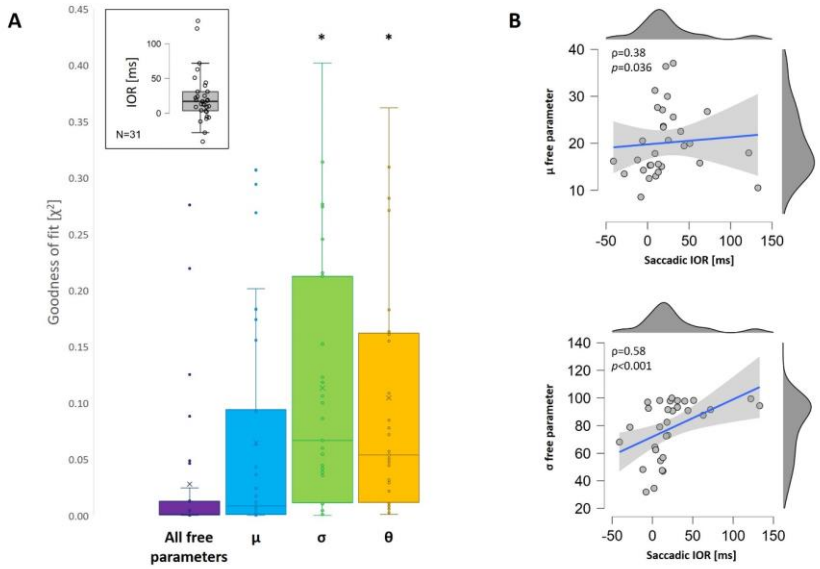

Figure 4: Saccadic IOR effect is explained by the Slope parameter. A. The goodness of fit of the All free parameters model (purple) significantly differed from the Gaussian noise free parameter model (σ, green) and the Threshold free parameter model (θ, yellow) (Repeated measures ANOVA p<.001, post hoc tests p<.001 and p<.001). The fit of the Slope free parameter model (μ, blue) and the All free parameters model is equivalent (Bayesian paired samples T-Test, overlapping & non-overlapping BF in favor of the interval-null=2.3 & 12.0 respectively), suggesting that the μ parameter differs between Return and Non-return conditions. Inset: The saccadic IOR effect of the subjects included in the modeling. B. Saccadic IOR effect is positively correlated with the μ parameter (top, Spearman **ρ**=0.38, p=0.036) and the σ parameter (Spearman **ρ**=0.58, p<0.001). Grey areas denote CI.

TMS effect on model goodness of fit

Bourgeois et al. (2013a, 2013b) tested the effects of repetitive TMS perturbation over four cortical regions on saccadic and manual IOR. Because RT analysis revealed there was a significant TMS effect only in the manual response modality, we focused on the effect of TMS on the modelling of manual IOR. We separately analysed the effect of TMS perturbation over the right IPS which led to a diminished manual IOR across the visual field (Bourgeois et al., 2013b), and TMS perturbation over the right TPJ, the left IPS and the left TPJ which only affected manual IOR when targets were presented on the right side, or did not affect IOR at all (Bourgeois et al., 2013a, 2013b).

TMS perturbation over left IPS, left TPJ and right TPJ hampers models' goodness of fit nonspecifically

We first explored the general effect of TMS perturbation over left IPS, left TPJ and right TPJ, on the goodness of fit of manual IOR models. In these regions, model goodness of fit post TMS stimulation was significantly worse than pre TMS (repeated measures ANOVA, TMS main effect: $F_{(1,18)}=4.75$, $p=0.04$, $\eta^2=0.05$; see figure 4). TMS perturbation did not differ across regions (TMS*Region interaction: $F_{(2,18)}=0.10$, $p=0.9$) or model parameters (TMS*modelling parameter interaction: $F_{(3,54)}=1.93$, $p=0.14$), suggesting a nonspecific TMS perturbation effect, not culminating in an IOR decrease (note again that our trial selection procedure, intended to maximise modelling robustness, differed from that of Bourgeois et al. (2013a, 2013b) and limited the subtlety of the effects we could observe; see Statistical analysis in the Methods section).

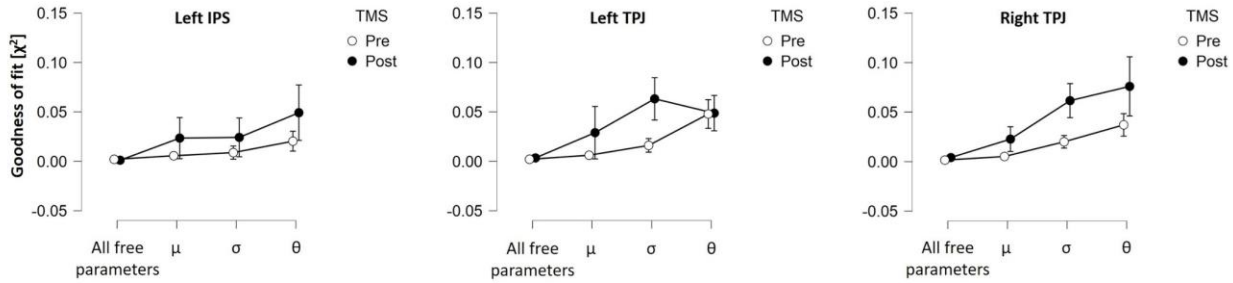

Figure 5: TMS stimulation perturbs model goodness of fit nonspecifically without affecting manual IOR across the visual field. In three cortical regions: left IPS, left TPJ and right TPJ, TMS perturbation did not affect manual IOR at all or only in one side of space. In these regions, model goodness of fit post-TMS stimulation was significantly worse than pre-TMS (repeated measures ANOVA, TMS main effect, $p=0.04$). TMS perturbation did not differ across regions (TMS*Region interaction $p=0.9$) or model parameters (TMS*Modeling parameter interaction $p=0.14$), suggesting a nonspecific TMS perturbation effect, not culminating in an IOR decrease. Error bars represent SE.

TMS perturbation over right IPS is explained by the slope parameter

Comparing the goodness of fit of accumulator models for the Return and Non Return conditions before and after TMS perturbation over the right IPS shows a significant effect of TMS (Durbin test, TMS effect: $F_{(7,48)}$=3.83 ,*pF*=0.002; see Figure 6). We next tested which parameter accounts best for the perturbed RT differences post TMS stimulation. The perturbed RT difference between Return and Non-return locations was best explained by the Slope (μ) parameter (Friedman test, $\chi^2_{(3)}$=11.07, *p*=0.011, Kendall's W=0.32, Conover's post hoc tests comparing μ free, σ free and θ free models to All free parameters model: *p*=0.27, *p*=0.015, *p*=0.012, respectively). Equivalence Bayesian Paired Samples t-test showed that there was anecdotal evidence supporting the equivalence of the fit between the μ free model and the All free parameters model (overlapping-hypothesis BF in favor of the interval-null, 1.33; non overlapping-hypothesis BF in favor of the interval-null, 1.68). These results suggest that TMS effect over right IPS might be mediated by the perturbation of the rate of the accumulation of evidence, but not through a change in decision threshold.

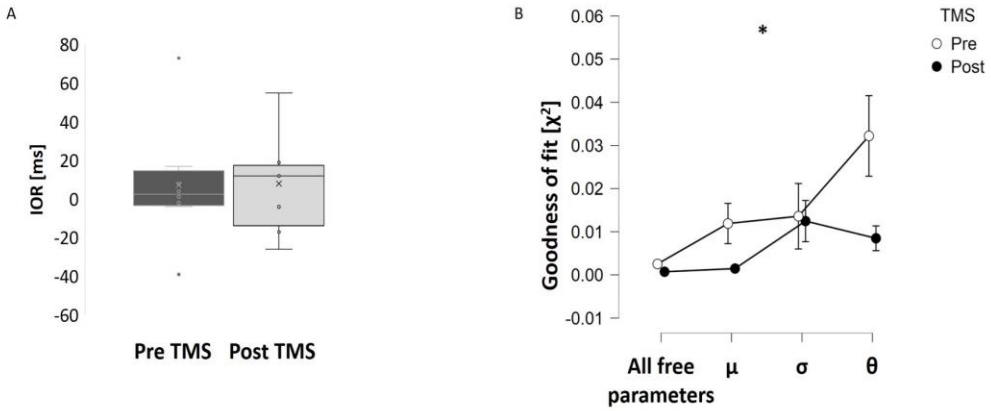

Figure 6: TMS perturbation over right IPS affects manual IOR and models' goodness of fit. A. IOR effect pre TMS stimulation (dark grey) and post TMS IOR (light grey). B. The goodness of fit of manual IOR models pre TMS perturbation (white circles) significantly differs from the fit post TMS (black circles; Durbin test, TMS effect *pF*=0.002). Post TMS, the perturbed Return-Non return RT difference is best explained by the Slope parameter (μ; Friedman test, *p*=0.011, Conover's post hoc test comparing μ free, σ free and θ free models to All free parameters model: *p*=0.27, *p*=0.015, *p*=0.012, respectively). Error bars represent SE.

Discussion

Does IOR attenuate processes at the sensory level, or does it influence motor programming? Behavioral evidence suggests that the sensory attenuation of stimulus-related responses may be automatic and non-motor, because it occurs independently of whether an eye or hand response is required, or whether the validity of the cues elicits reduced or increased reaction times (see, e.g., Lupiáñez et al., 2004; Posner & Cohen, 1984). Studies on the neurophysiological substrate of IOR in humans and non-human primates have led to similar conclusions. Inhibition of sensory cortical responses has been observed using an event-related potential IOR task (McDonald et al., 1999) and in response to repeated stimuli using a non-RT, delayed match to sample tasks both in the PPC (Steinmetz et al., 1994; Steinmetz & Constantinidis, 1995) and in the inferior temporal cortex (Miller et al., 1991). This suggests that it is a ubiquitous response property throughout a variety of brain areas. In the oculomotor sub-cortical system and in SC in particular, neuronal recordings have shown correlations between inhibition of the early sensory neuronal activity in SC and IOR behavior across experimental sessions and on a trial by trial basis within a single session (Dorris et al., 2002). All these reduced stimulus-related responses are compatible with a sensory-attentional account of IOR. Despite all these results, there is still debate on whether certain additional motor components of IOR remained valid or not (Ivanoff & Klein, 2001; Taylor & Klein, 2000). Mechanistically, a signal-to-noise ratio reduction of the sensory response applied to previously attended objects or regions of a scene is one way to explain IOR. This process would ensure that an initially salient region of the scene might not continue to have this status in time. Neurophysiologically, across multiple primary sensory areas, when a sudden stimulus appears at a position outside the receptive field (RF), lateral inhibition dominates the responses inside the RF (Pouget et al. 2005; Schall and Hanes 1993). When sequential stimulations are presented, RF responses are modulated by lateral inhibition. More precisely, the lateral inhibition following the first stimulation exceeded the termination of the stimulus by about 200ms and is therefore suitable not only for stimulus competition but also for supporting attentional capture (Lev-Ari et al., 2020). Despite this evidence, our understanding of the complete mechanisms and neurophysiological substrates of IOR remains sparse and fragmentary (Dorris et al., 2002).

Here, we tackled this mechanistic question by using a modelling strategy relating RTs to mathematical parameters mimicking the different stages of the neural processes leading to manual or saccadic responses (Carpenter & Williams, 1995; Gold & Shadlen, 2007; Pouget et al., 2009). By exploring the rate of accumulation of evidence toward a decision threshold, our results show that with either manual or saccadic responses, IOR mainly depended on a modulation of the slope of evidence accumulation. The ability of a simplistic stochastic accumulator model such as LATER to account for IOR effects in a quantitative manner may have important implications. Altered IOR may occur after CNS damage (Bartolomeo et al., 1999; Bourgeois et al., 2012; Sapir et al., 1999; Vivas et al., 2006), in psychiatric conditions (Mushquash et al., 2012), or upon neuromodulation of specific brain areas (Bourgeois et al., 2013b). Examining the underlying

parameters of the RT distributions may give novel and interesting insight into these deficits and brain functions rather than simply reporting IOR amplitude or time of occurrence, and can reasonably be expected to be a more direct reflection of the underlying neural processes. In the oculomotor domain, saccade-related neurons in FEF, SC, and Lateral Intraparietal cortex (LIP) are thought to be responsible for sensori-motor transformation (Coles et al., 1997; Everling & Munoz, 2000; Schall, 2019), and may therefore be relevant nodes of the IOR network. A strength of our model is its ability to predict IOR behavior. It represents a simple and robust way of conceptualizing IOR in the specific contexts of a target-target paradigm, and of TMS-mediated interference.

Variability between individuals is a common observation in IOR effect in humans and animals and also occurred in the group of human subjects tested here. We found that the variability in individual saccadic IOR scores was correlated with the Gaussian noise and the rate of accumulation parameters captured by the model. Additionally, the TMS conditions in our experiments indicate that intra-individual RT variability is larger post-TMS. Our findings indicate that individual RT variability in IOR is an important estimate of possible processes taking place during sensory selection. The robustness of modelling approaches depends also on the quantity of data modelled (number of subjects and input trials). This led us to adopt an inclusive trial-selection procedure, that on the other hand limited the subtlety of the effects we could study (e.g., collapsing left-sided and right-sided targets conditions together).

Our current results do not support Klein and Redden's (2018) proposal that "input" forms of IOR occur when the oculomotor system is suppressed (e.g., in manual IOR), and are mainly modulated by the ventral cortical visual stream; "output" forms of IOR may instead be observed when the reflexive oculomotor system is not suppressed (e.g., saccadic IOR), and depend on the activity of the dorsal visual stream. Our present evidence, obtained by modelling the results of a target-target paradigm with either manual or saccadic responses, indicated instead that both manual and saccadic IOR mainly depended on a modulation of the rate of evidence accumulation, whose likely neural correlates implicate fronto-parietal networks important for orienting of attention. In the oculomotor domain, saccade-related neurons in FEF, SC, and Lateral Intraparietal cortex (LIP) are thought to be responsible for the sensori-motor transformation (Coles et al., 1997; Everling & Munoz, 2000; Mushquash et al., 2012; Schall, 2019), and were shown to be relevant nodes of the IOR network (Mirpour et al., 2009, 2019). The involvement of these cortical regions in both saccadic and manual IOR was highlighted in the FORTIOR model (Seidel Malkinson & Bartolomeo, 2018), which postulates that both manual and saccadic IOR arise from reverberation of activity within priority maps of the frontoparietal circuit linking FEF and IPS. According to the FORTIOR model, differences between the readout capacities of the manual and saccadic effector systems when reading the output of the FEF-IPS circuit may then lead to the dissociations between saccadic and manual IOR. For example, the saccade system seems to be more encapsulated (i.e., less prone to interference and illusions) than the manual response system, and relies on a representation that accumulates visual information and location errors over

shorter time windows than the representation used for controlling hand movements (Lisi & Cavanagh, 2015, 2017).

The enthusiasm about the neurophysiological approach to track IOR effect is somewhat difficult to reconcile with the small changes in response times found in IOR manipulations (but see Dorris et al., 2002). Yet, to make it truly useful, the approach would ideally benefit from modelling hypotheses that are strong enough to be tested, rejected or validated. In this vein, converging evidence for the importance of these circuits in IOR comes from the effect of TMS-mediated interference on IOR upon stimulation of the right, but not of the left, intraparietal sulcus (Bourgeois et al., 2013a, 2013b). Our present modelling evidence confirms that TMS given on right IPS interferes with IOR-related parameters. Further studies involving single neuron recordings within parietal and prefrontal brain areas will be required to disentangle the dynamics and network extent of IOR generation.

Acknowledgements

This work was supported by ANR through ANR-16-CE37-0005 and ANR-10-IAIHU-06.

References

Bartolomeo, P., Chokron, S., & Siéroff, E. (1999). Facilitation instead of inhibition for repeated right-sided events in left neglect. *Neuroreport*, *10*(16), 3353–3357.

Bartolomeo, P., & Seidel Malkinson, T. (2019). Hemispheric lateralization of attention processes in the human brain. *Current Opinion in Psychology*, *29*, 90–96.

Bartolomeo, P., Siéroff, E., Decaix, C., & Chokron, S. (2001). Modulating the attentional bias in unilateral neglect: The effects of the strategic set. *Experimental Brain Research. Experimentelle Hirnforschung. Experimentation Cerebrale*, *137*(3/4), 424–431.

Berlucchi, G. (2006). Inhibition of return: a phenomenon in search of a mechanism and a better name. *Cognitive Neuropsychology*, *23*(7), 1065–1074.

Berlucchi, G., Di Stefano, M., Marzi, C. A., Morelli, M., & Tassinari, G. (1981). Direction of attention in the visual field as measured by a reaction time paradigm. *Behavioural Brain Research*, *2*(2), 244–245.

Bourgeois, A., Chica, A. B., Migliaccio, R., Thiebaut de Schotten, M., & Bartolomeo, P. (2012). Cortical control of inhibition of return: Evidence from patients with inferior parietal damage and visual neglect. *Neuropsychologia*, *50*(5), 800–809.

Bourgeois, A., Chica, A. B., Valero-Cabre, A., & Bartolomeo, P. (2013a). Cortical control of Inhibition of Return: Exploring the causal contributions of the left parietal cortex. *Cortex; a Journal Devoted to the Study of the Nervous System and Behavior*, *49*(10), 2927–2934.

Bourgeois, A., Chica, A. B., Valero-Cabre, A., & Bartolomeo, P. (2013b). Cortical control of inhibition of return: Causal evidence for task-dependent modulations by dorsal and ventral parietal regions. *Cortex; a Journal Devoted to the Study of the Nervous System and Behavior*, *49*(8), 2229–2238.

Brown, S. D., & Heathcote, A. (2008). The simplest complete model of choice response time: linear ballistic accumulation. *Cognitive Psychology*, *57*(3), 153–178.

Carpenter, R. H., & Williams, M. L. (1995). Neural computation of log likelihood in control of saccadic eye

movements. *Nature*, *377*(6544), 59–62.

Coles, M. G., Lynch, J. C., Richer, F., Achin, A., Schall, J. D., & Hanes, D. P. (1997). Neurons and reaction times [Review of *Neurons and reaction times*]. *Science*, *275*(5297), 142–143; author reply 144–145. science.sciencemag.org.

Dorris, M. C., Klein, R. M., Everling, S., & Munoz, D. P. (2002). Contribution of the primate superior colliculus to inhibition of return. *Journal of Cognitive Neuroscience*, *14*(8), 1256–1263.

Dorris, M. C., & Munoz, D. P. (1998). Saccadic probability influences motor preparation signals and time to saccadic initiation. *The Journal of Neuroscience: The Official Journal of the Society for Neuroscience*, *18*(17), 7015–7026.

Duncan Luce, R. (1986). *Response Times: Their Role in Inferring Elementary Mental Organization*. OUP USA.

Everling, S., & Munoz, D. P. (2000). Neuronal correlates for preparatory set associated with pro-saccades and anti-saccades in the primate frontal eye field. *The Journal of Neuroscience: The Official Journal of the Society for Neuroscience*, *20*(1), 387–400.

Gold, J. I., & Shadlen, M. N. (2007). The neural basis of decision making. *Annual Review of Neuroscience*, *30*, 535–574.

Gronau, Q. F., Ly, A., & Wagenmakers, E.-J. (2019). Informed Bayesian t-tests. *The American Statistician*, 1–14.

Ivanoff, J., & Klein, R. M. (2001). The presence of a nonresponding effector increases inhibition of return. In *Psychonomic Bulletin & Review* (Vol. 8, Issue 2, pp. 307–314). https://doi.org/10.3758/bf03196166

Jasp Team. (2020). *JASP (Version 0.12)[Computer software]*.

Klein, R. M. (1988). Inhibitory tagging system facilitates visual search. *Nature*, *334*(6181), 430–431.

Klein, R. M. (2000). Inhibition of return. *Trends in Cognitive Sciences*, *4*(4), 138–147.

Klein, R. M., & Redden, R. S. (2018). Two “inhibitions of return” bias orienting differently. *Spatial Biases in Perception and Cognition*, 295–306.

Lev-Ari, T., Zahar, Y., Agarwal, A., & Gutfreund, Y. (2020). Behavioral and neuronal study of inhibition of return in barn owls. *Scientific Reports*, *10*(1), 7267.

Lisi, M., & Cavanagh, P. (2015). Dissociation between the Perceptual and Saccadic Localization of Moving Objects. *Current Biology: CB*, *25*(19), 2535–2540.

Lisi, M., & Cavanagh, P. (2017). Different spatial representations guide eye and hand movements. *Journal of Vision*, *17*(2), 12.

Ludwig, C. J. H., Farrell, S., Ellis, L. A., & Gilchrist, I. D. (2009). The mechanism underlying inhibition of saccadic return. *Cognitive Psychology*, *59*(2), 180–202.

Lupiáñez, J. (2010). Inhibition of return. In *Attention and Time* (pp. 17–34). https://doi.org/10.1093/acprof:oso/9780199563456.003.0002

Lupiáñez, J., Decaix, C., Siéroff, E., Chokron, S., Milliken, B., & Bartolomeo, P. (2004). Independent effects of endogenous and exogenous spatial cueing: inhibition of return at endogenously attended target locations. *Experimental Brain Research. Experimentelle Hirnforschung. Experimentation Cerebrale*, *159*(4), 447–457.

Lupiáñez, J., Klein, R. M., & Bartolomeo, P. (2006). Inhibition of return: Twenty years after. *Cognitive Neuropsychology*, *23*(7), 1003–1014.

MacInnes, W. J. (2017). Multiple Diffusion Models to Compare Saccadic and Manual Responses for Inhibition of Return. *Neural Computation*, *29*(3), 804–824.

Maylor, E. A., & Hockey, R. (1985). Inhibitory component of externally controlled covert orienting in visual space. *Journal of Experimental Psychology. Human Perception and Performance*, *11*(6), 777–787.

McDonald, J. J., Ward, L. M., & Kiehl, K. A. (1999). An event-related brain potential study of inhibition of

return. *Perception & Psychophysics*, *61*(7), 1411–1423.

Miller, E. K., Gochin, P. M., & Gross, C. G. (1991). Habituation-like decrease in the responses of neurons in inferior temporal cortex of the macaque. In *Visual Neuroscience* (Vol. 7, Issue 4, pp. 357–362). https://doi.org/10.1017/s0952523800004843

Mirpour, K., Arcizet, F., Ong, W. S., & Bisley, J. W. (2009). Been there, seen that: a neural mechanism for performing efficient visual search. *Journal of Neurophysiology*, *102*(6), 3481–3491.

Mirpour, K., Bolandnazar, Z., & Bisley, J. W. (2019). Neurons in FEF Keep Track of Items That Have Been Previously Fixated in Free Viewing Visual Search. *The Journal of Neuroscience: The Official Journal of the Society for Neuroscience*, *39*(11), 2114–2124.

Mushquash, A. R., Fawcett, J. M., & Klein, R. M. (2012). Inhibition of return and schizophrenia: a meta-analysis. *Schizophrenia Research*, *135*(1-3), 55–61.

Noorani, I. (2014). LATER models of neural decision behavior in choice tasks. *Frontiers in Integrative Neuroscience*, *8*, 67.

Posner, M. I., & Cohen, Y. (1984). Components of visual orienting. In H. Bouma & D. Bouwhuis (Eds.), *Attention and performance X: Control of language processes* (pp. 531–556.). Erlbaum.

Posner, M. I., Rafal, R. D., Choate, L. S., & Vaughan, J. (1985). Inhibition of return: Neural basis and function. *Cognitive Neuropsychology*, *2*, 211–228.

Pouget, P., Logan, G. D., Palmeri, T. J., Boucher, L., Paré, M., & Schall, J. D. (2011). Neural basis of adaptive response time adjustment during saccade countermanding. *The Journal of Neuroscience: The Official Journal of the Society for Neuroscience*, *31*(35), 12604–12612.

Pouget, P., Stepniewska, I., Crowder, E. A., Leslie, M. W., Emeric, E. E., Nelson, M. J., & Schall, J. D. (2009). Visual and motor connectivity and the distribution of calcium-binding proteins in macaque frontal eye field: implications for saccade target selection. *Frontiers in Neuroanatomy*, *3*, 2.

Rafal, R., Egly, R., & Rhodes, D. (1994). Effects of inhibition of return on voluntary and visually guided

saccades. *Canadian Journal of Experimental Psychology = Revue Canadienne de Psychologie Experimentale*, *48*(2), 284–300.

Ratcliff, R., & Smith, P. L. (2004). A comparison of sequential sampling models for two-choice reaction time. *Psychological Review*, *111*(2), 333–367.

Sapir, A., Soroker, N., Berger, A., & Henik, A. (1999). Inhibition of return in spatial attention: direct evidence for collicular generation. *Nature Neuroscience*, *2*(12), 1053–1054.

Satel, J., Wilson, N. R., & Klein, R. M. (2019). What Neuroscientific Studies Tell Us about Inhibition of Return. *Vision (Basel, Switzerland)*, *3*(4). https://doi.org/10.3390/vision3040058

Schall, J. D. (2019). Accumulators, Neurons, and Response Time. *Trends in Neurosciences*, *42*(12), 848–860.

Seidel Malkinson, T., & Bartolomeo, P. (2018). Fronto-parietal organization for response times in inhibition of return: The FORTIOR model. *Cortex; a Journal Devoted to the Study of the Nervous System and Behavior*, *102*, 176–192.

Steinmetz, M. A., Connor, C. E., Constantinidis, C., & McLaughlin, J. R. (1994). Covert attention suppresses neuronal responses in area 7a of the posterior parietal cortex. *Journal of Neurophysiology*, *72*(2), 1020–1023.

Steinmetz, M. A., & Constantinidis, C. (1995). Neurophysiological evidence for a role of posterior parietal cortex in redirecting visual attention. *Cerebral Cortex* , *5*(5), 448–456.

Taylor, T. L., & Klein, R. M. (2000). Visual and motor effects in inhibition of return. *Journal of Experimental Psychology. Human Perception and Performance*, *26*(5), 1639–1656.

Usher, M., & McClelland, J. L. (2001). The time course of perceptual choice: the leaky, competing accumulator model. *Psychological Review*, *108*(3), 550–592.

Vivas, A. B., Humphreys, G. W., & Fuentes, L. J. (2006). Abnormal inhibition of return: A review and new data on patients with parietal lobe damage. *Cognitive Neuropsychology*, *23*(7), 1049–1064.